Original scientific paper

DEVELOPMENT OF A PROCEDURE FOR INCREASING THE ACCURACY OF THE RECONSTRUCTION AND TRIANGULATION PROCESS OF THE CRANIAL VAULT GEOMETRY FOR ADDITIVE MANUFACTURING

Paweł Turek, Grzegorz Budzik

Faculty of Mechanical Engineering and Aeronautics, Rzeszów University of Technology, Poland

ORCID iDs: Paweł Turek   https://orcid.org/0000-0002-5926-4815
       Grzegorz Budzik   https://orcid.org/0000-0003-3598-2860

Abstract. *CT scanners installed in clinics used different slice thicknesses, which usually produce data with an anisotropic structure of voxels. The low visual quality results are due to the discontinuous interpolation between neighboring voxels, resulting in a very "blocky" appearance of the reconstructed surfaces (stair-step artifact). This structure can also directly affect the volume, geometry, and linear accuracy of digital and physical 3D models. The article presents a method that improves the design of cranial vault models for additive manufacturing after the staircase artifact has occurred. The research was performed on 14 different patients (seven males and seven females). Changing the slice thickness from 2.4 mm to 4.8 mm generated over 90% errors in reconstructing the cranial vault area in the range of 0.830 mm +/- 1.364 mm (mean deviation +/- expanded uncertainty) for males and 0.780 mm +/- 1.338 mm for females. To increase the spatial resolution of the digital imaging data, an interpolation process was performed on 2D radiographic images. After using the data interpolation procedure (Lanczos filter), deviations were mainly in the range of 0.465 mm +/- 1.038 mm for males and 0.328 mm +/- 0.842 mm for females. The last stage of the improved process involved mesh optimization. Utilizing Laplacian smoothing surface and isotropic polygonal remesh, this procedure decreased global error, especially in regions with high curvatures. Over 90% of the analyzed points after using the Lanczos filter and optimization mesh procedure are within the range of 0.338 mm +/- 1.014 mm for males and 0.301 mm +/- 0.806 mm for females.*

Key Words: *Reverse Engineering, Triangulation, Cranial Vault, Accuracy, Interpolation, Additive Manufacturing*

1. INTRODUCTION

Traditional modeling of elements and parts of machines is carried out using computer-aided systems, which are presently widely used in designing and manufacturing industrial products [1-3]. The accuracy of the manufactured models is verified using contact [4, 5] and optical measurement systems [6-8]. Thanks to the development of coordinate measuring systems [9, 10], data processing systems [11], and modern manufacturing techniques [12, 13], it is possible to obtain the geometry of any object which does not have technical documentation [10, 11, 14], including a geometric model which matches the anatomy of soft or hard tissues [14-16]. The geometry of a piece of tissue or an entire organ is used in tissue engineering [17], surgery planning [18], surgical templates [19], and the manufacturing of implants and prostheses [19-21]. Models of anatomical structures are mainly used in orthopedics [22, 23], maxillofacial surgery[18-20], and cranioplasty [24, 25].The leading causes of bone defects in the cranial vault area are swelling of the skull bones, infection of the bone flap, and decompression operations in the case of uncontrolled swelling of the brain substance. To avoid the risk of postoperative complications, it is necessary to accurately design [26-28] and manufacture the implant or bone defect [24, 25]. Modern implants for cranioplasty must meet several requirements, including biocompatibility, and sterility.

Each stage of the reconstruction affects an object's dimensional and geometric accuracy. However, the contribution of each step to the final error remains unclear. The selection of the CT scanner type [14, 29], measurement parameters (e.g., tube potential or current) [29, 30], and image reconstruction parameters (e.g., voxel size, slice thickness, or convolution kernel) [29-32] plays an essential role in the further modeling process based on digital imaging data (DICOM). Then, a chosen anatomical structure is separated from the DICOM data by applying various segmentation methods, based mainly on detecting edges and identifying image areas with some standard features [31, 33]. Computer systems can visualize volumetric data in a three-dimensional geometry using, e.g., the Marching Cube (MC) and Delaunay algorithm [14]. Final models are mainly manufactured using additive techniques [16, 34, 35].

Due to the difficulties resulting from the estimation of errors at the acquisition and reconstruction stages of the geometry of anatomical structures from DICOM data, scientists are currently trying to conduct several studies in this area [31-33, 36]. The most common assessment is the deviation in linear dimensions. The process is carried out using a caliper [37], measuring arm [38], or coordinate measuring machine [39] on the natural bone structure provided by medical institutions. Then, the realistic bone model is digitalized using the CT systems [37, 39]. Based on the obtained results, the change in linear dimension is assessed, which occurred at the acquisition and reconstruction stages of the geometry, using a tomographic diagnostic system to the data obtained on the same research model using a caliper, coordinate measuring machine, or measuring arm. In assessing 3D geometry errors related to the acquisition data, geometry reconstruction, and manufacturing stage, a structural light scanner was also used [40].

A challenging task is to improve the accuracy of digital model geometry at the stage of acquisition and data processing. It is impossible to obtain the highest spatial resolution during CT measurements owing to the need to protect the patient's health. Low spatial resolution is related to data characterizing a voxel where the slice thickness is incomparably more significant than the pixel dimensions [29, 30]. During data analysis characterized by irregular voxel dimensions (a partial volume effect artifact is created), there is a limited

possibility of successfully segmenting the data. The poor quality of mapping the geometry is due to the lack of continuity of data interpolation, which in turn generates the block structure of the standard tessellation language (STL) model (which produces the so-called stair-step artifact) [14, 32]. This artifact can directly affect the volume, geometry, and linear accuracy of digital and physical 3D models. The anisotropic nature of many datasets can be a severe quality issue for image analysis and visualization techniques. In addition to this, reconstruction algorithms such as an MC or Delaunay have their limitations. The generated triangle mesh based on algorithms contains many errors, which are related, among others, to inverted normal vectors, twisted surfaces, or overlapping triangles. These reconstructed geometries require additional mesh editing and optimizing [41-43].

The skull is a significant bone tissue, being a natural shield for the delicate structure of the brain. From an anatomical point of view, there is a discernible difference between the male and female skulls. The forehead is slightly sloping and receding in males, while in females, the forehead is vertical. Additionally, the cranial vault is more rounded in males, while the cranial vault is flattened in females [44]. The differences in the anatomical structure of the male and female skulls are most noticed in the sagittal and coronal planes. Unfortunately, partial volume effect artifacts in 2D images significantly hinder the correct segmentation of geometry outlines in the presented planes [45]. Imaging thick CT layers can produce a stair-step artifact on the 3D model. Working on 3D models of male or female skulls containing geometry errors, the process of CAD modeling of the skull defect is significantly more difficult. This aspect results from the difficulty of correctly reconstructing the realistic outline of the implant and the problem of fitting it to the entire skull [46]. Currently, no methods of improving the accuracy of the reconstruction and triangulation process of cranial vault geometry after stair-step artifact has occurred are available. The article presents DICOM data processing and geometry reconstruction methods that may enhance the design of cranial vault models and extend the methodology of analytical accuracy determination at the data processing stage.

2. METHOD

The research was performed on 14 different patients. In this group, there were seven males aged from 41 to 72 years old and seven females aged from 34 to 69 years old. DICOM data were obtained for all patients on the Siemens Somatom Sensation Open 40 scanner installed in the Regional Clinical Hospital No. 1 at the Frederic Chopin in Rzeszow, with a commonly used scanning protocol for the cranial area. Patients were scanned twice using different slice thicknesses to carry out the research process (Tab. 1) The increase in the layer thickness influenced the creation of partial-volume effect artifacts in the 2D image data. Reconstruction geometry was performed in the Amira software. In the segmentation process of the cranial vault, a lower threshold of 200 HU was used. The final surface was saved in STL format (Fig. 1).

Table 1 Scanning protocol

| Name of parameters | Somatom Sensation 40 (sequence mode) | |
	Value of parameters (first measurements)	Value of parameters (second measurements)
kV	120	120
mAs	380	380
Rotation time	1 second	1 second
Acquisition	24 × 1.2 mm	24 × 1.2 mm
Slice collimation	1.2 mm	1.2 mm
Kernel	H31s	H31s
Matrix size	512 × 512	512 × 512
Pixel size	0.4 mm × 0.4 mm	0.4 mm × 0.4 mm
Slice thickness	2.4 mm	4.8 mm

To increase the spatial resolution of the DICOM data, and to limit the influence of the artifact partial volume effect, an interpolation process was applied to the traverse plane performed for the second measurement. This is a process of creating a new synthetic pixel from adjacent pixels so that it is optically best-matched to the transformed image. The interpolation process is often included to convert data to an isotropic grid.
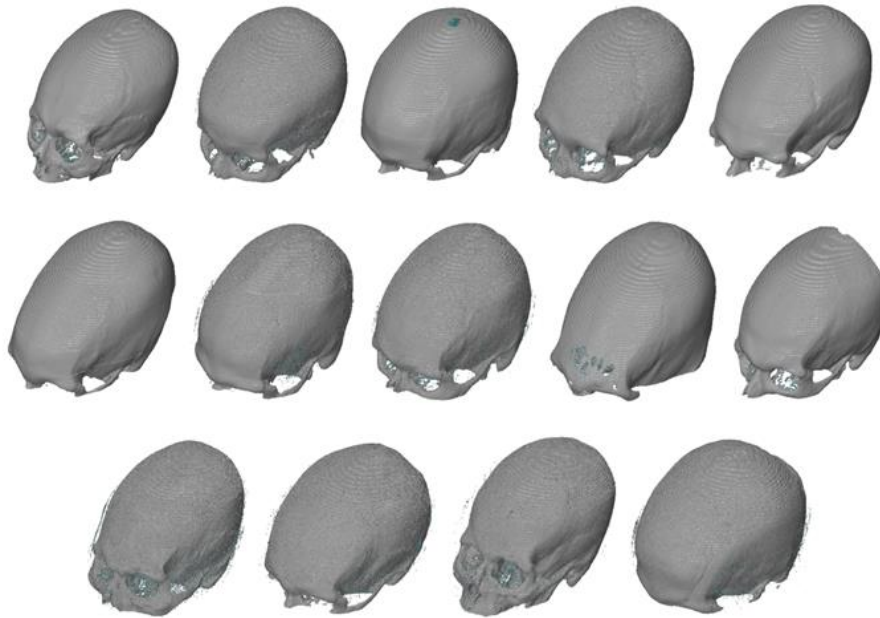
Fig. 1 The surface representing cranial models of 14 patients

There are many algorithms available that can accomplish the interpolation [47-49], but they differ in their quality and computational effort. However, the current research shows that the Lanczos filter is more effective than other methods in minimizing the

impact of the stair-step artifact [50, 51]. The algorithm considers neighboring points in 4 x 4, 6 x 6, and 8 x 8 blocks. Lanczos convolution kernel $L(x)$ is defined as:

$$L(x) = \begin{cases} \sin c(x)\sin c(x/a)\, if \; -a < x < a, \\ \qquad 0 \qquad\qquad otherwise. \end{cases} \tag{1}$$

The parameter is a positive integer, usually 2 or 3, that specifies the kernel size. The Lanczos kernel has 2 to - 1 lobe: a positive one in the center and a - 1 alternating positive and negative cams on each side. This filter has excellent characteristics. When correctly applied, it yields a perfect equilibrium between detail preservation (sharpness) and smoothness. This method produces slight overshoot, high edge sharpness, good signal continuity in the smooth region, and decreases artifact partial-volume effect. The interpolation procedure using the Lanczos filter did improve the accuracy of reconstruction to reformat a voxel's structure from 0.4 mm × 0.4 mm × 4.8 mm. to the iso-voxel 0.4 mm × 0.4 mm × 0.4 mm using (Fig. 2). Then, the DICOM data were subjected to data segmentation and geometry reconstruction under the same methods and parameters as the non-processed models.
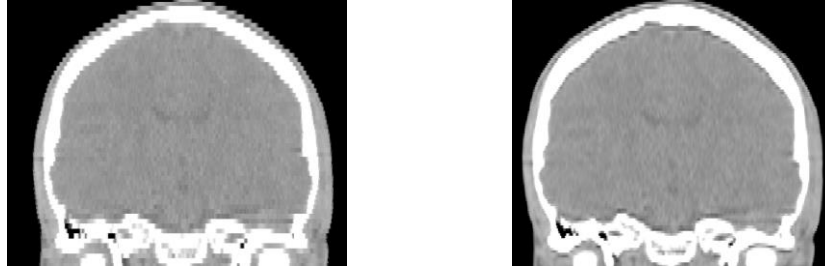

Fig. 2 The view on 2D image of the first patient, voxel size: 0.4 mm × 0.4 mm × 4.8 mm (left), and improved using the Lanczos filter (right)

Moreover, the process involved mesh optimization. The MC algorithm generates holes, aliases, saw-toothed paths within the voxel connection, and increased global error, especially in the regions with high curvatures (Fig. 3a). Using variable-density triangular meshes, the optimization procedure was performed (Fig. 3b). This procedure involves two steps:
- Laplacian smoothing surface by shifting its vertices. Each synthetic vertex is shifted to the average position of its neighbors. The Laplace function is the sum of the squares of the lengths of the edges having a common node:

$$f(x,y) = \sum_{i=1}^{k} \left((x-x_i)^2 + (y-y_i)^2 \right) \tag{2}$$

where k is the number of neighbors nodes.

Node optimization is performed for each mesh node. The new node coordinates (x', y') are calculated from the formulas:

$$x' = \frac{1}{k}\sum_{i=1}^{k} x_i \quad y' = \frac{1}{k}\sum_{i=1}^{k} y_i \tag{3}$$

▪ Remesh the surface by creating small dense triangles in the high curvature region and large sparse triangles in the low curvature region in regard to the coronal and sagittal plane by using an isotropic vertex placement algorithm.
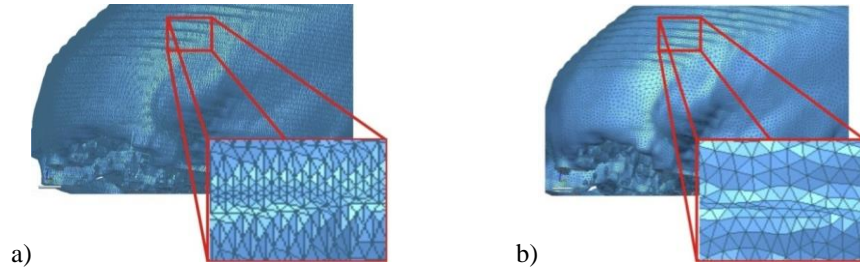

a)   b)

Fig. 3 The optimization procedure of STL mesh, a) before, b) after

In the process of assessing the accuracy of reconstruction (first step) and triangulation (second step), a model with a voxel structure of 0.4 mm × 0.4 mm × 2.4 mm (first measurements) was selected as the reference model for comparison and the model accuracy assessment (Fig. 4). This model was chosen because it obtained a higher spatial resolution than the model with a voxel structure of 0.4 mm × 0.4 mm × 4.8 mm.
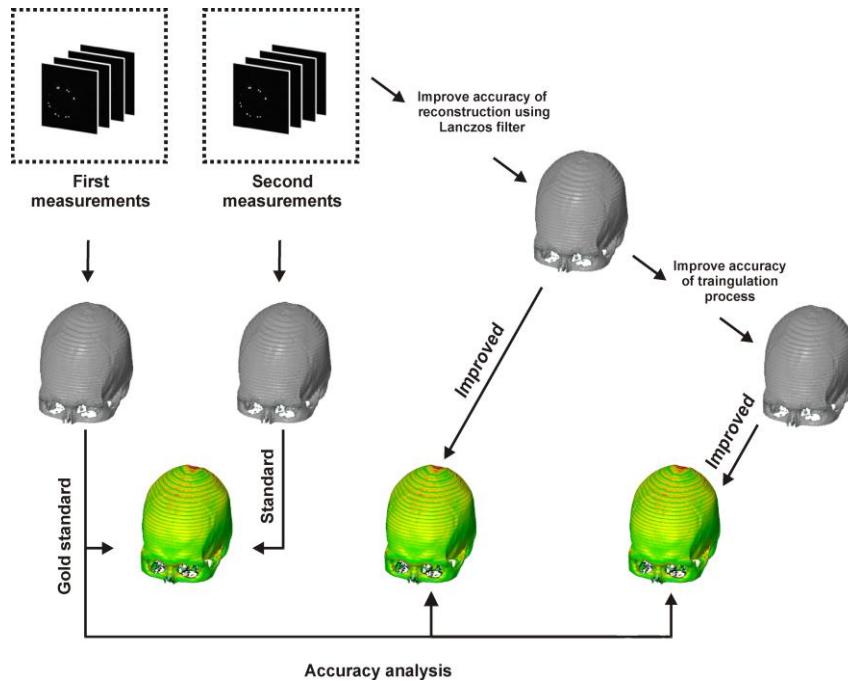

Fig. 4 The comparison process

The comparison process was performed using the best-fit method. This algorithm is most appropriate for analyzing deviations in the models with complex shapes. A best-fit alignment is an iterative process that minimizes the square of the distance between the nominal and measured data to converge on a solution. Adjustment of point clouds is made using the best-fit to an accuracy of 0.001 mm.

3. RESULTS AND DISCUSSION

To examine the accuracy of geometry reconstruction, the models of the 14 cranial vaults with a voxel size of 0.4 mm × 0.4 mm × 4.8 mm were compared and improved using a Lanczos filter (first step) and triangulation procedure (second step) with the same cranial vault based on modeling with a voxel size of 0.4 mm × 0.4 mm × 2.4 mm (the gold standard). The statistical parameters and distributions of the reconstructed models from DICOM data are presented in Figs. 5-7, Tab. 2 and 3.

In the case of averaged results presented in Figs. 5a, 6a, and 7a, the artifact partial-volume effect significantly increases the positive deviations to the gold standard model. The poor quality of geometry reconstruction using the MC algorithm is due to the lack of continuity of data interpolation, which generates the model's block structure (stair-step artifact). For an averaged seven male cranial vaults, the deviations are mainly in the range between 0.357 mm and 0.714 mm, and for seven females, in the range between 0.714 mm and 1.071 mm. The averaged results for 14 patients confirm that more than half of the analyzed deviations range from 0.357 mm to 1.071 mm. There are also places where negative deviations can be observed (for males – 15 % and for females 8 % of analyzed points). Over 90 % of the analyzed points are within the range of 0.830 mm +/- 1.364 mm for males and 0.780 mm +/- 1.338 mm for females. In the case of skew and kurtosis, all distribution is more peaked than a Gaussian distribution (Leptokurtic distribution) and characterized by medium asymmetry (value close to 0.5).

Considering the averaged results obtained after using the Lanczos filter, an increase in the accuracy of the cranial vault was observed (Fig. 5b, Fig. 6b, and Fig. 7b). The artifact's partial-volume effect has been minimized (Fig. 2). By improving the spatial resolution of the DICOM data, an increase in the number of points representing the geometry of the cranial vault was observed. The concentration of deviations has changed. For male and female cranial vaults, the deviations are mainly between 0 mm and 0.357 mm values, respectively 26.80 % and 38.10 %. However, there has been an increase in negative deviations, mainly in the range between -0.357 mm and 0 mm. Over 90 % of the analyzed points are within the range of 0.465 mm +/- 1.038 mm for males and 0.328 mm +/- 0.842 mm for females. In the case of skew and kurtosis, the parameter values were decreased. All distributions are Leptokurtic, characterized by small (for males) and medium (for females) asymmetry. The obtained averaged statistical parameters for 14 patients are consistent with the average results for males and females.

After optimizing the triangle mesh, the errors of the structure, which resulted from the use of the MC algorithm, were removed (Fig. 3). Additionally, the number of points representing the geometry of the cranial vault was reduced, which was doubled due to the Lanczos interpolation method (Fig. 5c, Fig. 6c, and Fig. 7c).

Fig. 5 Histogram representing the average results of the 7th males, a) not improved, b) improved using interpolation, c) improved using the interpolation and triangulation procedure

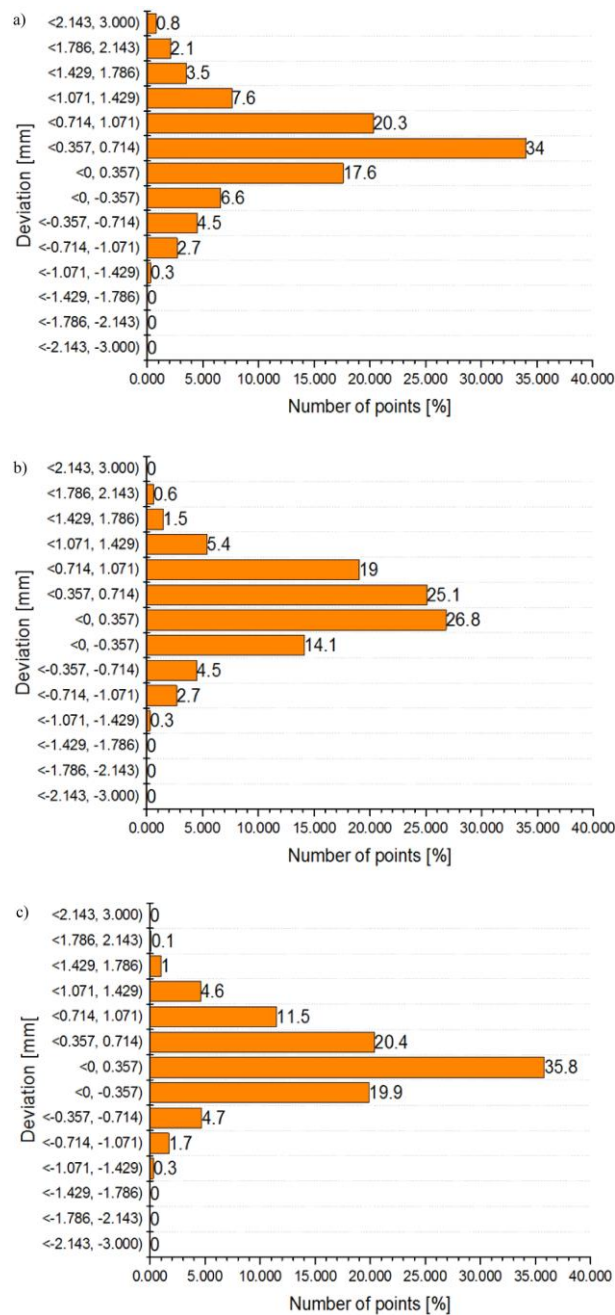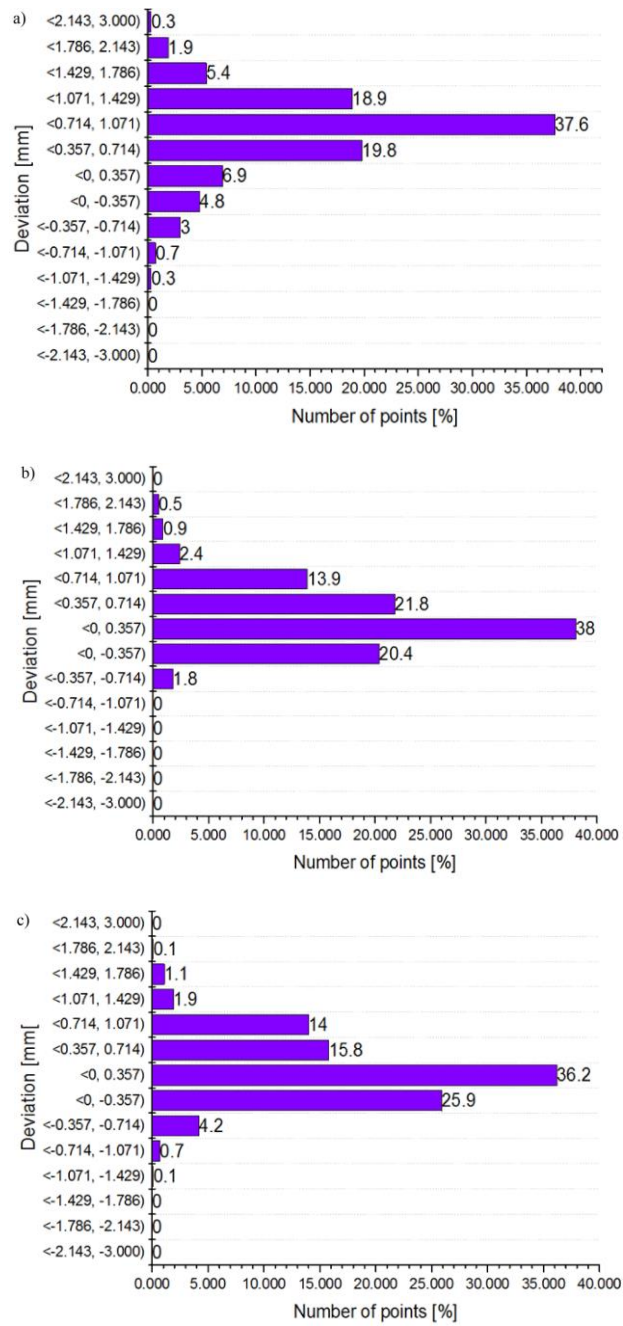**Fig. 6** Histogram representing the average results of the 7ᵗʰ females, a) not improved, b) improved using the interpolation, c) improved using the interpolation and triangulation procedure
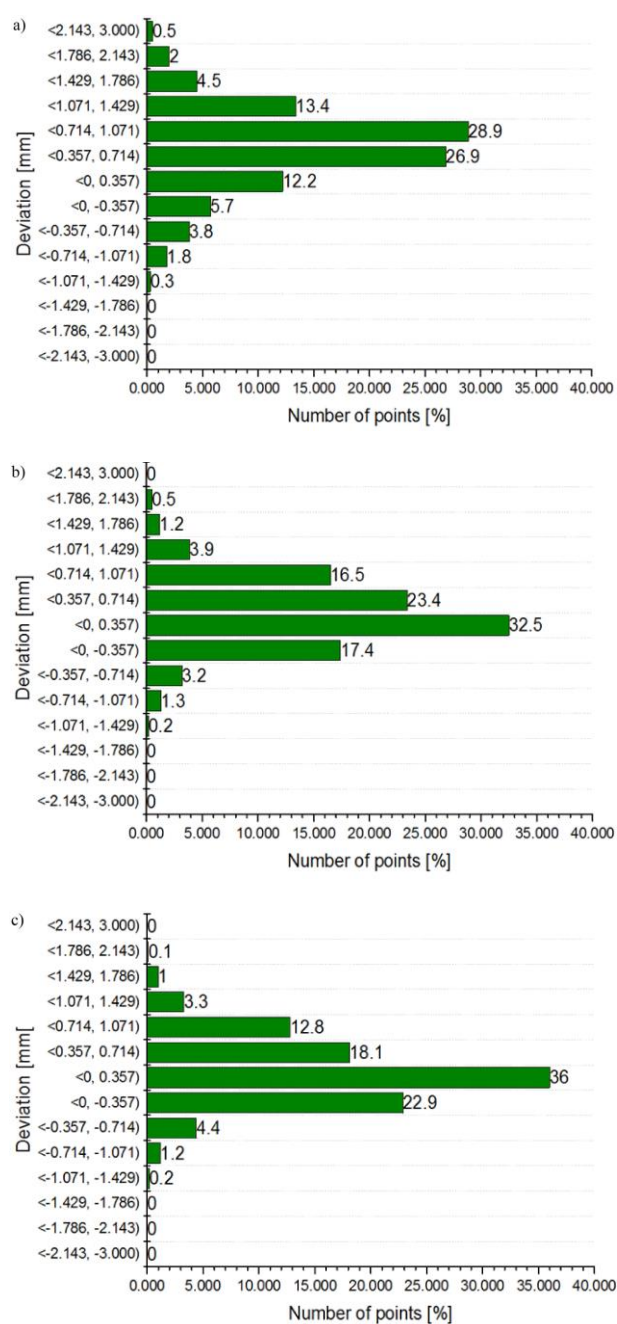
Fig. 7 Histogram representing the average results of the 14th patients, a) not improved, b) improved using interpolation, c) improved using the interpolation and triangulation procedure

Table 2 Statistical results of not improved models

Parameters	Not improved		
	Male	Female	Average
Number of points	233335	220757	227046
Mean deviation [mm]	0.830	0.780	0.805
Standard deviation [mm]	0.682	0.669	0.676
Skewness	0.335	0.472	0.404
Kurtosis	4.709	4.559	4.634

After using the mesh optimization process, the obtained number of points is similar to the one that defines the model not subjected to any optimization procedure. There was an increase in points within a tolerance of +/- 0.350 mm. For males, the percentage of points within the tolerance of +/- 0.350 mm is approximately 56%, and for females, about 62%. Compared to the models not subjected to the procedure, the males were around 22% and females around 12 % (Fig. 5a, Fig. 6a, and Fig. 7a). Over 90% of the analyzed points after using Lanczos filter and optimization mash procedure are within the range of 0.338 mm +/- 1.014 mm for males and 0.301 mm +/- 0.806 mm for females.

Table 3 Statistical results of improved models

Parameters	Improved using interpolation			Improved using interpolation and triangulation		
	Male	Female	Average	Male	Female	Average
Number of points	380345	406661	393503	207527	295238	251383
Mean deviation [mm]	0.465	0.328	0.397	0.338	0.301	0.320
Standard deviation [mm]	0.519	0.421	0.470	0.507	0.403	0.455
Skewness	0.235	0.407	0.321	0.206	0.210	0.208
Kurtosis	3.802	4.201	4.002	4.432	4.060	4.246

4. CONCLUSION

The influence of the Lanczos filter on the accuracy of reconstruction cranium geometry is very similar for the 14 presented patients (seven males and seven females). When using the Lanczos filter, one may observe an improvement in the accuracy of the reconstruction of the cranial vault geometry. Also, the time of segmentation was shortened. The presented optimization mesh procedure adopted the resolution of triangles according to the local curvature. Large triangles are used to define planar regions in this procedure whereas small triangles are used for curved areas. Thanks to this, the process of generating a triangle mesh has been accelerated, without losing the accuracy of representation in the areas characterized by colossal complexity. Additionally, thanks to carrying out the process of mesh optimization, the structure of the digital model for 3D printing has been directly prepared. The presented results prove that it is possible to increase the accuracy of the reconstruction and triangulation process of anatomical models' geometry at this stage of data editing. Additionally, further development of the procedure is also planned, especially at the stage of numerical processing of DICOM data, by using the deep learning method in segmentation. These methods should allow for a further reduction of the time needed for preparation of models.

REFERENCES

1. Reddy, E.J., Venkatachalapathi, N., Rangadu, V.P., 2018, *Development of an approach for Knowledge-Based System for CAD modeling*, Materials Today: Proceedings, 5(5), pp. 13375-13382.
2. Camba, J.D., Contero, M., Company, P., 2016, *Parametric CAD modeling: An analysis of strategies for design reusability*, Computer-Aided Design, 74, pp. 18-31.
3. Magdziak, M., 2020, *Determining the strategy of contact measurements based on results of non-contact coordinate measurements*, Procedia Manufacturing, 51, pp. 337-344.
4. Raja, V., Kiran, J.F., 2010, *Reverse Engineering—An Industrial Perspective*, Springer: New York, NY, USA.
5. Barbero, B.R., Ureta, E.S., 2011, *Comparative study of different digitization techniques and their accuracy*, Comput Aided Design, 43(2), pp. 188-206.
6. Gdula, M.; Burek, J., Żyłka, Ł., Płodzień, M., 2018, *Five-axis milling of sculptured surfaces of the turbine blade*, Aircraft Engineering and Aerospace Technology, 90(1), pp. 146-157.
7. Rokicki, P., Budzik, G., Kubiak, K., Dziubek, T., Zaborniak, M., Kozik, B., Bernaczek, J., Przeszłowski, Ł., Nowotnik, A., 2016, *The assessment of geometric accuracy of aircraft engine blades with the use of an optical coordinate scanner,* Aircraft Engineering and Aerospace Technology, 88(3), pp. 374-381.
8. Brajlih, T., Tasic, T., Drstvensek, I., Valentan, B., Hadzistevic, M., Pogacar, V., Balic, J., Acko, B., 2011, *Possibilities of using three-dimensional optical scanning in complex geometrical inspection.* Stroj Vestn J Mech Eng, 57(11), pp. 826-833.
9. Habrat, W., Zak, M., Krolczyk, J., Turek, P., 2018, *Comparison of geometrical accuracy of a component manufactured using additive and conventional methods,* In: Hamrol A, Ciszak O, Legutko S, (eds) Advances in manufacturing. Cham: Springer, pp. 765-776.
10. Dziubek, T., 2018, *Application of coordination measuring methods for assessing the performance properties of polymer gears,* Polimery, 63(1), pp. 49-52.
11. Urbanic, R.J., Elmaraghy, H.A., Elmaraghy, W.H, 2008, *A reverse engineering methodology for rotary components from point cloud data,* Int J Adv Manuf Tech, 37(11–12), pp. 1146-1167.
12. Baggi, E., 2009, *Reverse engineering applications for recovery of broken or worn parts and re-manufacturing: three case studies,* Adv Eng Softw, 40(6), pp. 407-418.
13. Gibson, I., Rosen, D., Stucker, B., 2014, *Additive Manufacturing Technologies*, Springer, New York, NY, USA.
14. Thompson, M.K., Moroni, G., Vaneker, T., Fadel, G., Campbell, R.I., Gibson, I., Bernard, A., Schulz, J., Graf, P., Ahuja, B., Martina, F., 2016, *Design for Additive Manufacturing: Trends, opportunities, considerations, and constraints,* CIRP Ann. Manuf. Technology, 65, pp. 737-760.
15. Preim, B., Bartz, D., 2007, *Visualization in Medicine: Theory, Algorithms, and Applications*, Morgan Kaufmann, San Francisco.
16. Bidanda, B., Bartolo, P., 2008, *Virtual Prototyping & Bio Manufacturing in Medical Applications*, Springer, New York, NY, USA.
17. Budzik, G., Turek, P., Dziubek, T., Gdula, M., 2020, *Elaboration of the measuring procedure facilitating precision assessment of the geometry of mandible anatomical model manufactured using additive methods*, Measurement and Control, 53(1-2), pp. 181-191.
18. Sun, W., Starly, B., Nam, J., Darling, A., 2005, *Bio-CAD modeling and its applications in computer-aided tissue engineering*, Comput-Aid Des, 37(11), pp. 1097-1114.
19. Pietruski, P., Majak, M., Swiatek-Najwer, E., Popek, M., Szram, D., Zuk, M., Jaworski, J., 2016, *Accuracy of experimental mandibular osteotomy using the image-guided sagittal saw*, Int J Oral Maxillofac Surg, 45(6), pp. 793-800.
20. Ciocca, L., Mazzoni, S., Fantini, M., Persiani, F., Baldissara, P., Marchetti, C., Scotti, R., 2012, *A CAD/CAM-prototyped anatomical condylar prosthesis connected to a custom-made bone plate to support a fibula free lap*, Med Biol Eng Comput, 50(7), pp. 743-749
21. Farias, T.P., Dias, F.L., Sousa, B.A., Galvão, M.S., Bispo, D., Pastl, A.C., 2013, *Prototyping: Major Advance in Surgical Planning and Customizing Prostheses in Patients with Bone Tumors of the Head and Neck*, Int. J. Clin. Med, 4(7), pp. 1–7.
22. Singh, S., Prakash, C., Ramakrishna, S., 2019, *3D printing of polyether-ether-ketone for biomedical application,* Eur. Polym. J, 114, pp. 234–248.
23. Montgomery, S.J., Kooner, S.S., Ludwig, T.E., Schneider, P.S., 2020, *Impact of 3D printed calcaneal models on fracture understanding and confidence in orthopedic surgery residents*, Journal of Surgical Education,77(2), pp. 472-478.
24. Chamo, D., Msallem, B., Sharma, N., Aghlmandi, S., Kunz, C., Thieringer, F.M., 2020, *Accuracy assessment of molded, patient-specific polymethylmethacrylate craniofacial implants compared to their 3D printed originals*, Journal of clinical medicine, 9(3), 832.

25. Kwarcinski, J., Boughton, P., Ruys, A., Doolan, A., Van Gelder, J., 2017, *Cranioplasty and craniofacial reconstruction: a review of implant material, manufacturing method and infection risk*, Applied sciences, 7(3), 276.
26. Korunovic, N., Marinkovic, D., Trajanovic, M., Zehn, M., Mitkovic, M., Affatato, S., 2019, *In silico optimization of femoral fixator position and configuration by parametric CAD model*, Materials, 12(14), 2326.
27. Stojkovic, M., Veselinovic, M., Vitkovic, N., Marinkovic, D., Trajanovic, M., Arsic, S., Mitkovic, M., 2018, *Reverse modelling of human long bones using T-splines-case of tibia*, Tehnicki Vjesnik, 25(6), pp. 1753-1760.
28. Turek, P., 2021, *Evaluation of the auto surfacing methods to create a surface body of the mandible model,* Reports in Mechanical Engineering, 3(1), pp. 46-54.
29. Rudek, M., Gumiel, Y.B., Canciglieri Jr, O., Asofu, N., Bichinho, G.L., 2018, *A CAD-based conceptual method for skull prosthesis modelling*, Facta Universitatis-Series Mechanical Engineering, 16(3), pp. 285-296.
30. Romans, L., 2018, *Computed Tomography for Technologists: A comprehensive text*, Lippincott Williams & Wilkins.
31. Alsleem, H., Davidson, R., 2013, *Factors affecting contrast-detail performance in computed tomography: A review*, Journal of Medical Imaging and Radiation Sciences, 44(2), pp. 62-70.
32. Van Eijnatten, M., van Dijk, R., Dobbe, J., Streekstra, G., Koivisto, J., Wolff, J., 2018, *CT image segmentation methods for bone used in medical additive manufacturing*, Medical engineering & physics, 51, pp. 6-16.
33. Budzik, G., Turek, P., Traciak, J., 2017, *The influence of change in slice thickness on the accuracy of reconstruction of cranium geometry*, Proceedings of the Institution of Mechanical Engineers, Part H: Journal of Engineering in Medicine, 231(3), pp. 197-202.
34. Van Eijnatten, M., Koivisto, J., Karhu, K., Forouzanfar, T.,Wolff, J., 2017, *The impact of manual threshold selection in medical additive manufacturing*, International journal of computer assisted radiology and surgery, 12(4), pp. 607-615.
35. Salmi, M., Paloheimo, K.S., Tuomi, J., Wolff, J., Mäkitie, A., 2013, *Accuracy of medical models made by additive manufacturing (rapid manufacturing)*, Journal of Cranio-Maxillofacial Surgery, 41(7), pp. 603-609.
36. Huotilainen, E., Jaanimets, R., Valášek, J., Marcián, P., Salmi, M., Tuomi, J., Wolff, J., 2014, *Inaccuracies in additive manufactured medical skull models caused by the DICOM to STL conversion process*, Journal of Cranio-Maxillofacial Surgery, 42(5), pp. e259-e265.
37. Van Eijnatten, M., Berger, F.H., De Graaf, P., Koivisto, J., Forouzanfar, T., Wolff, J., 2017, Influence of CT parameters on STL model accuracy, Rapid Prototyping Journal, 23(4), pp. 678-685.
38. Periago, D.R., Scarfe, W.C., Moshiri, M., Scheetz, J.P., Silveira, A.M., Farman, A.G., 2008, *Linear accuracy and reliability of cone beam CT derived 3-dimensional images constructed using an orthodontic volumetric rendering program*, The Angle Orthodontist, 78(3), pp. 387-395.
39. Szymor, P., Kozakiewicz, M., Olszewski, R., 2016, *Accuracy of open-source software segmentation and paper-based printed three-dimensional models*, Journal of Cranio-Maxillofacial Surgery, 44(2), pp. 202-209.
40. Primo, B.T., Presotto, A.C., De Oliveira, H.W., Gassen, H.T., Miguens Jr, S.A.Q., Silva Jr, A.N., Hernandez, P.A.G., 2012, *Accuracy assessment of prototypes produced using multi-slice and cone-beam computed tomography*, International journal of oral and maxillofacial surgery, 41(10), pp. 1291-1295.
41. Akmal, J.S., Salmi, M., Hemming, B., Teir, L., Suomalainen, A., Kortesniemi, M., Lassila, A., 2020, *Cumulative inaccuracies in implementation of additive manufacturing through medical imaging, 3D thresholding, and 3D modeling: A case study for an end-use implant*, Applied Sciences, 10(8), 2968.
42. Pinto, J.M., Arrieta, C., Andia, M.E., Uribe, S., Ramos-Grez, J., Vargas, A., Tejos, C., 2015, *Sensitivity analysis of geometric errors in additive manufacturing medical models*, Medical engineering & physics, 37(3), pp. 328-334.
43. Manmadhachary, A., Kumar, R., Krishnanand, L., 2016, *Improve the accuracy, surface smoothing and material adaption in STL file for RP medical models*, Journal of Manufacturing Processes, 21, pp. 46-55.
44. Nikita, E., Michopoulou, E., 2018, *A quantitative approach for sex estimation based on cranial morphology*, American journal of physical anthropology, 165(3), pp. 507-517.
45. Grassberger, M., Gehl, A., Püschel, K., Turk, E.E., 2011, *3D reconstruction of emergency cranial computed tomography scans as a tool in clinical forensic radiology after survived blunt head trauma—report of two cases,* Forensic science international, 207(1-3), pp. e19-e23.
46. Li, J., von Campe, G., Pepe, A., Gsaxner, C., Wang, E., Chen, X., Egger, J., 2021, *Automatic skull defect restoration and cranial implant generation for cranioplasty,* Medical Image Analysis, 73, 102171.

47. Msallem, B., Sharma, N., Cao, S., Halbeisen, F.S., Zeilhofer, H.F., Thieringer, F.M., 2020, *Evaluation of the dimensional accuracy of 3D-printed anatomical mandibular models using FFF, SLA, SLS, MJ, and BJ printing technology*, Journal of clinical medicine, 9(3), 817.
48. Thévenaz, P., Blu, T., Unser, M., 2000, *Image interpolation and resampling*, Handbook of medical imaging, processing and analysis, 1(1), pp. 393-420.
49. Lehmann, T.M., Gonner, C., Spitzer, K., 1999), *Survey: Interpolation methods in medical image processing*, IEEE transactions on medical imaging, 18(11), pp. 1049-1075.
50. Budzik, G., Turek, P., 2020, *The impact of use different type of image interpolation methods on the accuracy of the reconstruction of skull anatomical model*, Biomedical Engineering: Applications, Basis and Communications, 32(01), 2050008.
51. Budzik, G., Turek, P., 2018, *Improved accuracy of mandible geometry reconstruction at the stage of data processing and modeling*, Australasian physical & engineering sciences in medicine, 41(3), pp. 687-695.